Mapping soil Available Water Capacity spatially and temporally across the Adams' farm near Ungarra, Eyre Peninsula

Mark Thomas[1], Damian Mowat[1] and Jacob Giles[2]

[1] *CSIRO Agriculture and Food, Waite Campus; mark.thomas@csiro.au*
[2] *EP Ag Research, Port Lincoln*

Background

Dan Adams' farm, which is located near Cockaleechie and Ungarra on the Eyre Peninsula (EP), participates in the Resilient EP Smart Farms project by contributing one of the 'focus paddocks' known as "Tank". This paddock had a soil moisture probe installed in the ground during 2016.

Dryland farmers increasingly turn to soil moisture information to reduce decision-making uncertainty and maximise production opportunity for profit. Key decision support areas include strategic, including what to sow and when, as also tactical decisions including in-season choices like when (… or if) to apply N, or to market grain with increased confidence.

Soil moisture probe output can only be considered reliable for soils proximal to the sensor; strictly speaking the instrument is calibrated to *that soil* and *that soil* only. This is because soils vary spatially and with depth so simple extrapolation of sensor data from one site (soil) to another is problematic; the nature and rate of change is sometimes hard to predict with reliability, especially in landscapes that have complex soil arrangements.

Of all the soil components that contribute most to moisture retention in soils (e.g. available water capacity, AWC[1]), clay content in typical agricultural soils is the most dominant factor and so the patterns can have a very strong influence on soil-landscape variability. In practical terms this means that without advance knowledge on the farm soils, reliability of soil moisture sensor information diminishes and devalues at an unknown rate with increasing distance from the probe. To counter this, in an ideal world the farmer would deploy an array of sensors to cover a multitude soils that are probably present. However, because soil moisture sensors are not cheap, cost consideration shapes usage and so many farmers opt for a single on-farm installation.

The famer/advisor is then faced with the choice of where that sensor should be deployed. This decision is often built around accumulated knowledge of soil/yield patterns. Therefore the rationale for 'optimal' deployment may fall on the farmer's interest in the consistently best-, worst- or average-performing soils – or some other criteria important to the farmer. However, the 'optimal' is rarely

[1] The term AWC can often be used synonymously with plant available water capacity (PAWC). The PAWC estimate technically relates to the soil water availability for a crop-type for the whole rooting depth and integrates soil constraints like salinity and pH. In this pilot AWC is estimated for ≤ 1 m soil depth (depending on depth of soil core refusal and regardless of rooting depth) and does not integrate constraints.

achievable because of practical constraints to installation since on the working farm sensors can rarely be positioned far from the edge of the paddock to minimise disruption to farm operations. For example, the sensor control unit and peripherals need to be outside the cropped area to not disrupt operations traffic and to give unfettered access for checking and maintenance and deploying the sensor close to the edge of the paddock minimises disruption to crops if the senor needs to be accessed.

The purpose of this pilot study is to, firstly, map at mapping a granularity (~ scale) helpful to farming decision-making the AWC of soils across the whole of Adams farm using a modern soil mapping approach called digital soil mapping (DSM), and then secondly, use the soil moisture signal from the Tank soil moisture sensor to estimate by extrapolation the volumetric water content of soils across the farm. Were this to be reliable, the methodology could be used to assist at other farms that have a soil moisture sensor to support whole-of-farm farmer strategic and tactical decision-making. In itself, the AWC farm map will be a useful addition to the farmer's decision-making tool kit. The pilot study only draws off nationally available datasets so that if prospects for success are good it will be possible to extend the approach elsewhere.

Farm soils

The Adams farm boundary is presented in Figure 1. The cropped area of the farm covers approximately 400 Ha in an upland setting, and the landscape is characterised by low hills featuring low relief patterns of hillcrests, hillslopes, drainage depressions and footslopes. The soils are derived from very old Paleoproterozoic era intrusives rocks (gneissic granites and granodiorites) and much more recent - though nonetheless still old - Cenozoic era residual sediments from past alluvial deposits covering much of the present-day high ground. These deposits are subject to in-situ weathering. The source materials result in well-structured soils that are often rich in clay with texture contrast and gradational-type profiles, although lighter loam soils may also be present. The influence of weathering means that some soils contain ironstone gravels. Some soils derived from the intrusives may be rich in grit in layers or throughout the profile. In places a shallow (0.2 - 0.3 m) calcrete restricts soil depth, or the soils contain appreciable amounts of calcrete gravels and stones. Away from these areas soil depth is generally not restricted to a depth ≥1 m. Subsoils on the farm are typically alkaline (some very alkaline) and some may be sodic – particularly soils influenced by weathering of the intrusives.

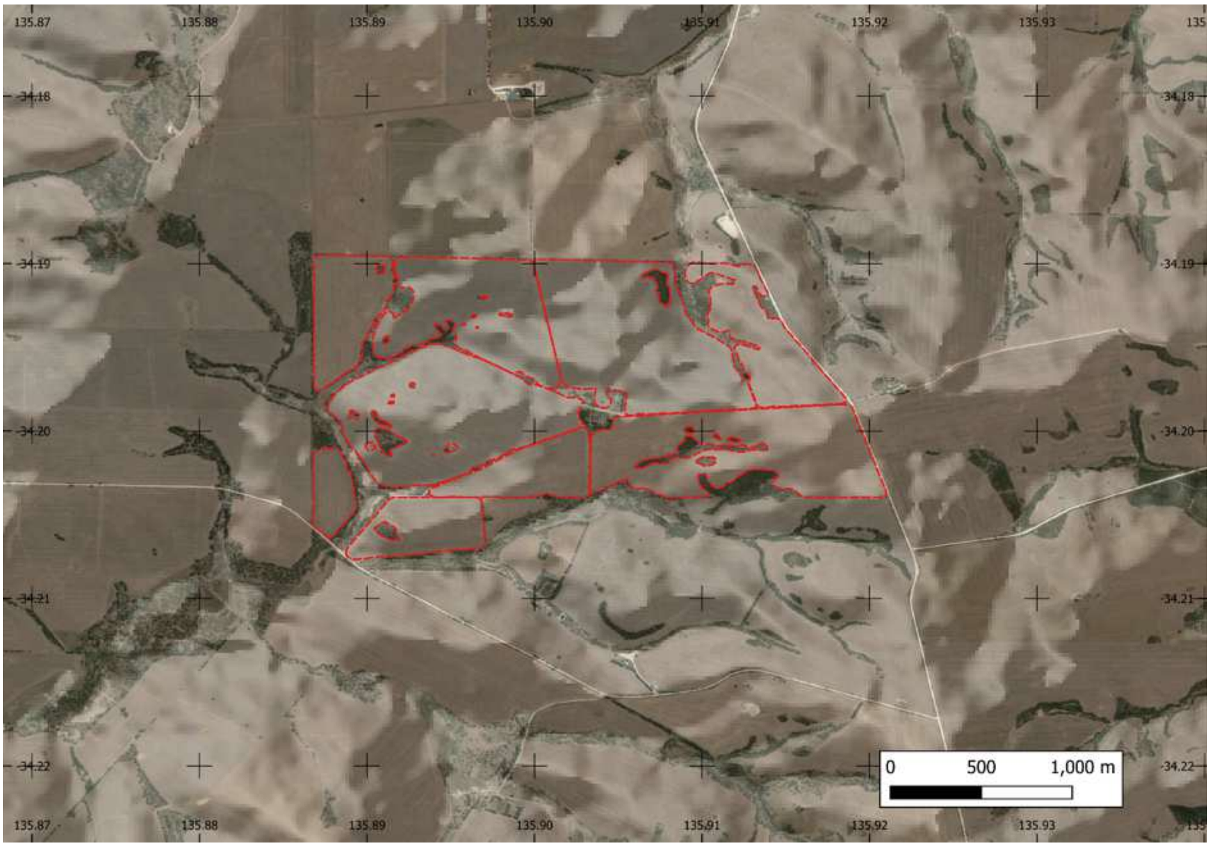

Figure 1 Adams farm extent including paddock boundaries (red lines) and artificial hill shading added to accentuate relief patterns

Methods

The first stage of the methodology involves devising a soil survey that is both pragmatic and efficient; efficient in terms covering the full range of soils in the farm soil-landscape within survey constraints. In-field sampling methodology is also described. The analytical suite of samples is described. Next, the DSM approach is discussed, including the evaluation of results. Finally, we discuss extrapolation and assessment of soil moisture signal from the Tank probe across the farm.

Survey design and soil sampling

Conceptual background

The key objective of soil survey design is to cover as much as possible of the soil continuum (i.e. variety, or types) in the study area with as little bias as possible. In practical operational terms, bias introduces inefficiencies in terms of over-sampling soils at the expense of others. Technically, bias skews surveyor (mental) and computer models by not equally covering – or even missing– important soils during formulating predictive models.

A survey comprising 25 sites was envisaged the maximum achievable during a working a working day. However, given the likelihood of attrition of sites because of access problems or running out of field time, a balance of >20 sites achieved was deemed acceptable enough to offer a reliable coverage of farm soils. Achieving 20 over the 400 Ha of farmland gives a sampling intensity of one sample per 20 Ha. This sampling intensity equates to moderately high (detailed) intensity survey (e.g. a sampling point support consistent with 1:25,000 scale mapping) and considered useful for farm planning (Gallant et al., 2008).

There are numerous survey design approaches (McKenzie et al., 2008) including surveying at expertly selected sites, on a grid or at random site. One method that 'forces' the design to cover the soil-landscape continuum applies stratification, which separates the soil-landscape based on clusters of 'similarness' and distributing the chosen number of sampling points equally within each cluster/stratum.

One effective method of clustering to define strata applies environmental correlation. This approach applies the principle that certain GIS layers relating to soils and landscapes spatially correlate to soil properties, i.e. they are soil property *covariates*. For example, the thorium (Th) gamma radiometric layer is a covariate for weathered soils; strong Th signals can therefore indicate the presence of deeper, less fertile soils (Wilford et al., 1997). Similarly, topographic wetness index (TWI) terrain analysis (Wilson and Gallant, 2000a) indicates patterns of water flows and persistence, hence is a covariate for soil thickness, soil hydrology and soil texture. Slope can serve as a covariate for soil depth. Covariates are discussed in Table 1.

Computer *k*-means analysis is an established method in soil survey for creating a map of *k-number* of statistical clusters from a coregistered stack of covariates (Burrough, 1989). The main principles of *k*-means analysis are that (i) '*k'* is an operator-determined number of clusters, and (ii) each *k*-means cluster generated is equally statistically variable – or discrete – as each of the other clusters. In practice, because clustering is based on covariates, all the user knows is that each cluster represents a coherent set of soil properties in the landscape, but what those properties are is not necessarily understood i.e. the cluster map is not a soil classification. However, expert visual coregistration of the cluster map with covariates in GIS can be a useful way of conceptually determining a range of general soil properties of clusters. The user-attribution of *k* is best done iteratively with expert knowledge guidance, and starts by matching a known level of soil-landscape complexity with a suitable number for *k*. For example, a non-complex landscape situation is likely to be better served by a small *k* whereas a complex situation may be better served by a larger *k* as there is more soil variability (i.e. types of soils) present.

Sources of covariates

Consistent with pilot objectives of ensuring that methodology can be extended throughout EP without barriers, covariates were derived from Australian public databases. The majority of covariates were collected from the Soil Landscape Grid of Australia (SLGA; Grundy et al., 2015) and the Sentinel remote sensing mission (Torres et al., 2012). The GIS rasters were unified to a 20 m ground resolution, and the SLGA's digital elevation model (DEM) used to derive additional terrain attributes if not already in the suite.

Implementing *k*-means clustering

The pilot used the freely available and powerful Quantum GIS (QGIS) GIS program (https://www.qgis.org/en/site/). This GIS supports the PAT (Precision Agriculture Tool) plugin developed by CSIRO (Ratcliff et al., 2020) that is also freely available. *k*-means clustering is part of one of the PAT modules and used in this pilot.

Numerous clustering iterations were implemented in PAT and assessed qualitatively and informed by field experience gained during a field reconnaissance and auxiliary information, including remote sensing, soil data, publications (Hall et al., 2009) and soil mapping (Maschmedt, 2000). The output considered the best representation of soil patterns was a 4-cluster solution shown in Figure 2, which was achieved using the 7 covariates presented in Table 1.

Table 1. Covariates, examples of soil property proxies/covariances and usage. Ticks indicate usage in the pilot.

Covariate	Examples of soil property proxies/covariances	Pilot usage	
		Clustering	Digital soil mapping
Radiometric K	Shallow(er) or rocky soils; rocks derived from shallow underlying geology (Wilford et al., 1997)	✓	✓
Radiometric Th	Deep(er), low fertility (leached) soils (Wilford et al., 1997)	✓	✓
Weathering Intensity Index	Separating deeply weathered, residual soils from shallow, unweathered soils (Wilford, 2012)	✓	✓
Focal Mean 300 m	Land surface relief patterns from an intermediate sized 300 m neighbourhood. Extenuates changes in slope and landform.	✓	
Prescott Index	Identification of soil leaching based on climate (aridity) moderated locally by slope aspect; high index values indicate poorly leached soils and possible presence of subsoil pans (Prescott, 1950)	✓	✓
Topographic Wetness Index	Areas of water accumulation and slow soil water transmission (leached, waterlogged/wet soils) and areas of water shedding (drier soils) (Gallant and Austin, 2012)	✓	✓
Slope	Shallow(er) versus deep(er) soils (Wilson and Gallant, 2000b)	✓	
Kaolin mineralogy	Weathered soils		✓
Smectite mineralogy	Fresher soils		✓
Illite mineralogy	Fresher soils		✓
Sentinel satellite short wave infrared (VV polarisation)	Land use and near surface soil moisture		✓
Sentinel satellite short wave infrared 2 (VH polarisation	Land use and near surface soil moisture		✓
Geology	Multiple soil attributes like mineralogy, texture		✓

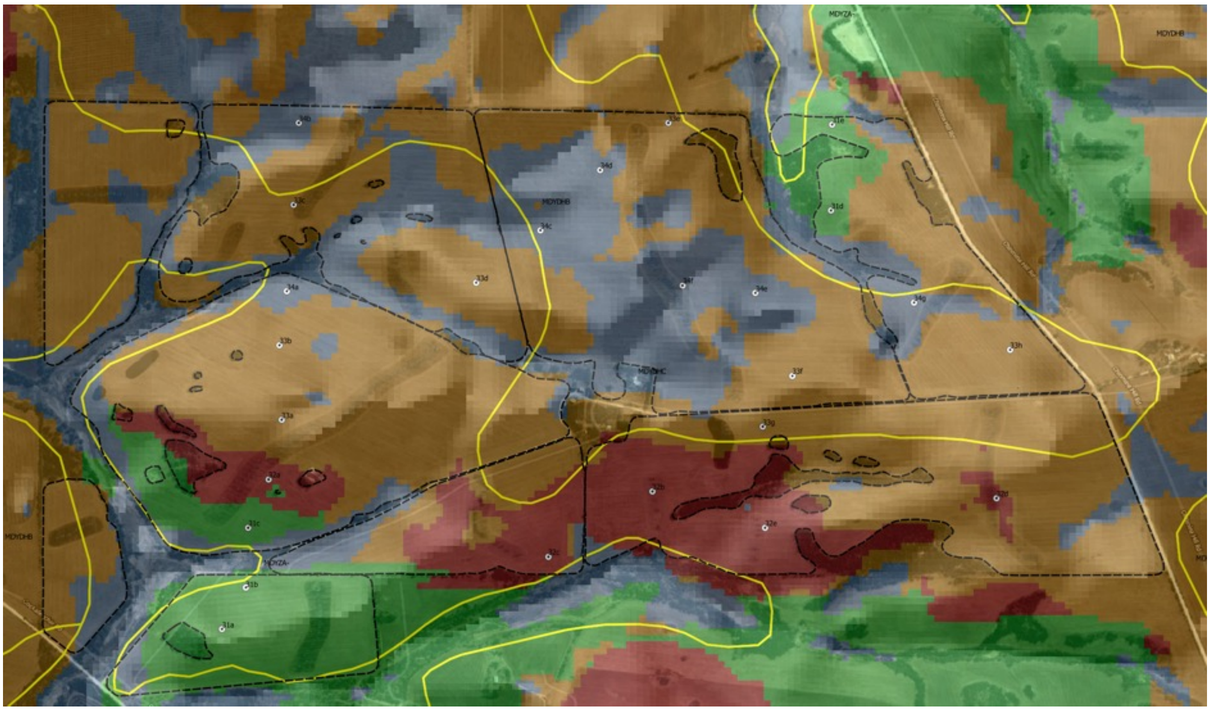

Figure 2. Adams farm 4-cluster k-means clustering solution. Planned sampling sites are shown (white dots)

An analysis of distribution of preliminary core AWC results[2] sub-setted according to the 4 clusters shown in Figure 2 taken at the sampling points is shown in Figure 3. This shows that apart from the cluster 4 (blue) that straddles all cluster distributions of AWC and a similar median to cluster 3 (yellow), the remaining clusters show reasonable separation. This indicates in terms of the AWC attribute at least, the survey design appears to have adequately fulfilled the objective of covering a variety of soils on the farm.

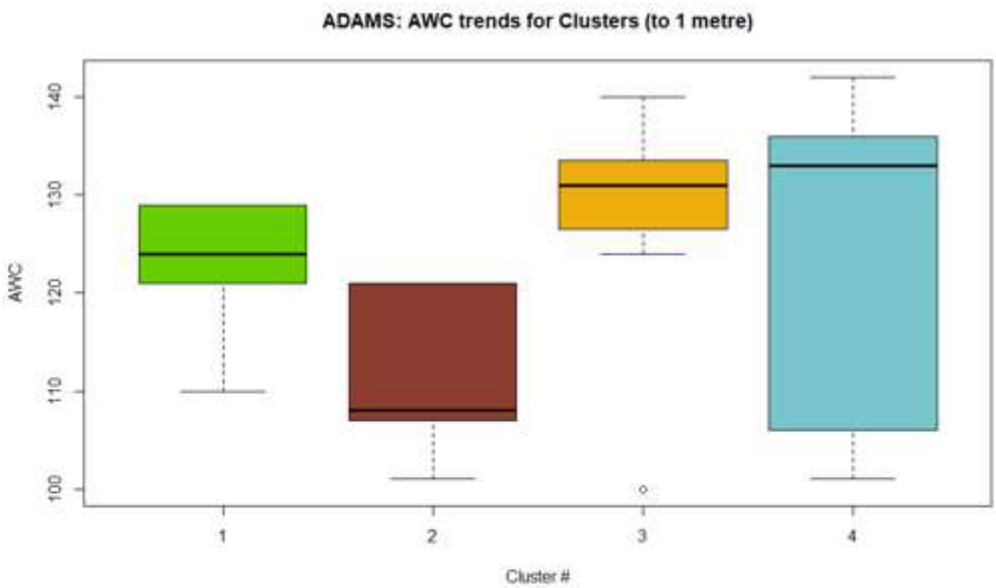

Figure 3. Boxplots of AWC size distributions at sampling points grouped by coloured cluster, as shown in Figure 2

Finding sampling sites

The method to select the 25 candidate survey sites involved distributing a proportionate amount of sites based on the area of land for each cluster. In this way cluster 1 was allocated 5 survey sites; cluster 2, 5 sites; cluster 3, 8 sites, and; cluster 4, 7 sites. Next, within these, sites were expertly

---

[2] Section: "Soil water retention and available water capacities"

assigned; wherever possible, sites were aligned into transects based on hillslope. Sampling in this way is beneficial in two ways: firstly, technical efficiencies are achieved by sampling down slope because soil variability is maximised tangential to slope. Secondly, practical efficiencies are achieved sequential sites being in closer proximity to one other ensuring field sampling time is maximised.

Soil sampling

A GPS was used to navigate to the sites shown in Figure 2. A 40-mm push tube corer was used to extract complete soil cores to a depth of 1 m or refusal. Two cores were collected at each site. The first was described at 0.2 m depth increments, each of which were bagged for physiochemical laboratory analyses. The second was divided into 0.1 m depth increments for laboratory water retention analysis (suction, pressure plate analyses). Twenty-two sites were achieved during the survey (Figure 4).

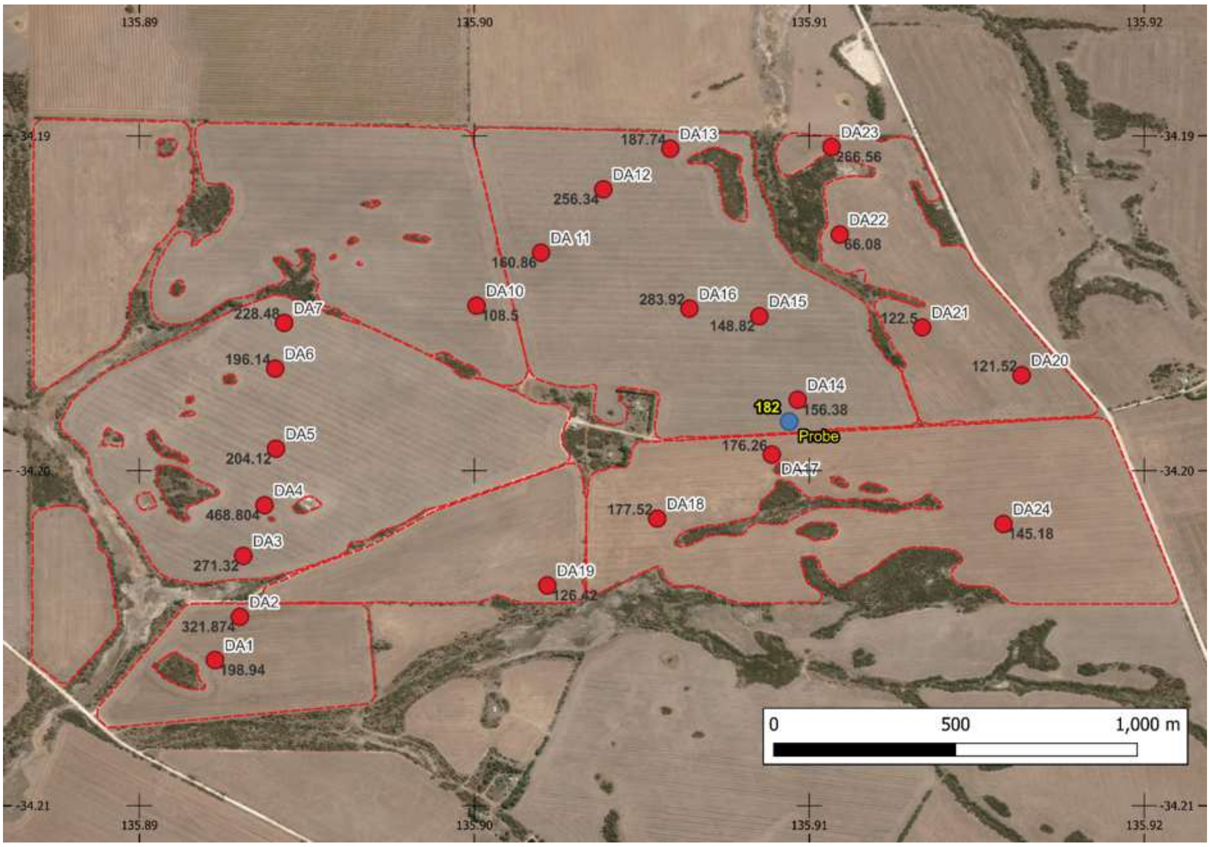

Figure 4. Distribution of the 22 sampling sites as red dots. White buffered label show site IDs and non-buffered label reflects DSM estimated AWC. (DSM see "Digital Soil Mapping" section). The blue dot locates the Tank soil moisture probe and the field characterisation PAWC (yellow with black buffer)

The Tank soil moisture probe is identified in Figure 4. The soil proximal to the probe has a field estimated PAWC of 182 mm. The probe is situated roughly equidistant from sampling sites DA14 and DA17 (80 and 120 m, respectively). DA14 has a DSM AWC estimate of 156 mm and DA17 has one at 176 mm. The Tank probe's PAWC is estimated to 1.2 m depth whereas the DSM estimates are to 1 m depth.

Soil analysis

Physiochemical

The <2 mm fraction was analysed for a conventional suite of analyses on the 0.2 m depth increment samples. The analyses included pH, salinity (EC), Ca, Mg, Na, K, as well as texture. Texture was analysed using mid infra-red (MIR) scanning. MIR can often vary in accuracy depending on the strength of calibration, and in situations where prediction uncertainty was high, particle size analysis was used.

Soil water retention and available water capacities

Available water capacity for the 0.1 m depth increment was analysed using methods in Cresswell (2002). The -15 bar pressure plate measurement is used to approximate the crop lower limit (CLL) and the -0.3 bar suction plate measurement is used to approximate the field drained upper limit (DUL). Conversion to volumetric water was estimated using bulk density data derived from a GIS intersection of the sampling points from the SLGA bulk density layers. Plots showing the upper (-0.3 bar) and lower (-15 bar) limits are shown in Appendix 1. The down profile AWC trends derived from the plate work are presented in Figure 8.

A whole profile AWC (to 1 m depth) for each of the 22 soils sampled was calculated by summing the 0.1 m increment AWC values and are shown in Figure 5. The mean AWC to 1 m depth for the value is 199 mm, with a standard deviation of 85.7 mm.

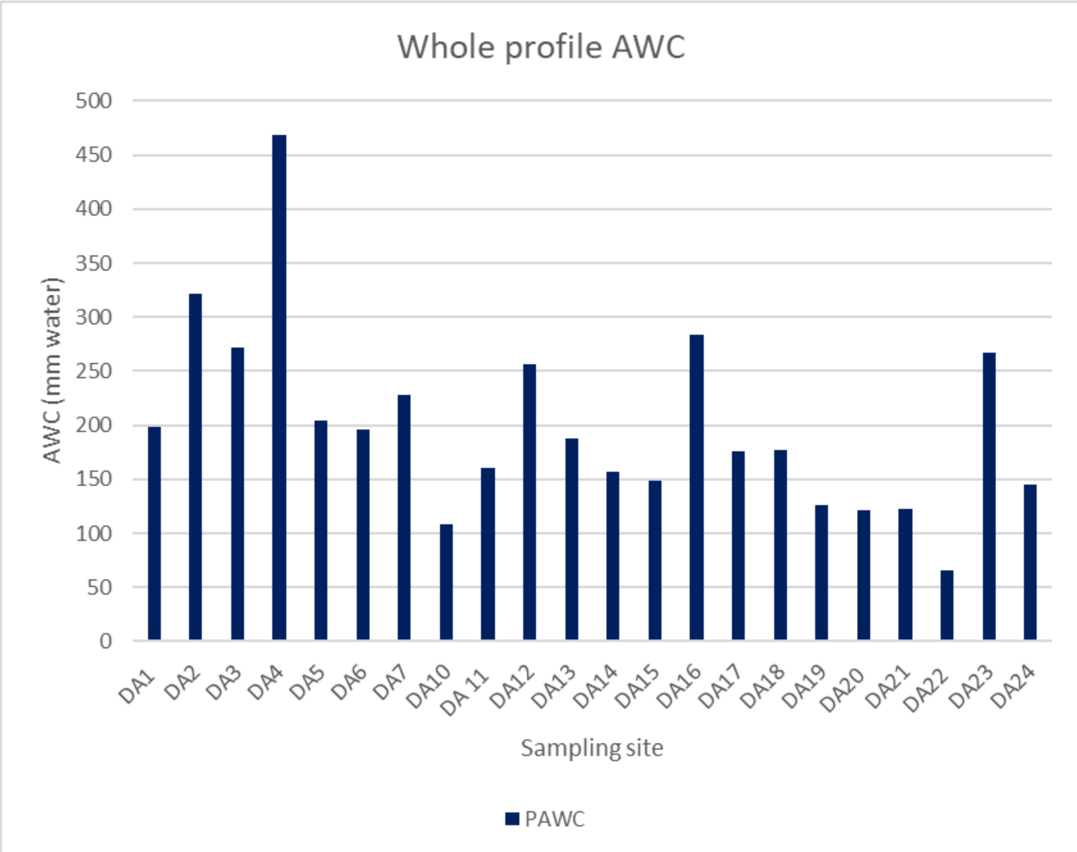

Figure 5. Whole profile (to 1 m) available water capacity for sampled soils

Digital soil mapping

The machine learning technique applies computer modelling to predict and map soil properties using DSM (McBratney et al., 2003). Many DSM approaches build and apply predictive models established from relationships between point-based soil observations (i.e. geolocated soil data) and covariates (McKenzie and Ryan, 1999), and are capable of predicting the distributions of soil properties at various depths. This pilot applied the commonly used “Cubist” algorithm implemented in the “DSMTools” app developed by CSIRO to remove adoption barriers.

Model set-up has numerous user options. These include the suite of covariates, and the way model ‘training’ is supported. Training is the process by which the predictive model is iteratively built from observations (i.e. the geolocated laboratory data from the sampling sites, here AWC) intersecting with values from the stack of covariates. The model is also tested, and there are two methods to do this. One option called ‘external’ validation is to withhold a selection (e.g. 20 %) of the observations, build the model with the remaining 80 %, and then validate the model with the withheld 20 %. One drawback of external validation is the withheld data is 'wasted', i.e. does not contribute to model building. An alternative option is to use 'internal' validation, which randomly withholds a pre-set number of data points for validation (e.g. 20 %), builds the model with the remaining 80 %, tests against the 20 %, and then finally returns the 20 % back into the set of observations. The technique repeats this numerous times (e.g. tens to thousands of times) according to user preference. Statistical reliability is reported on accumulated results of each repeat. The benefit of internal validation is that all observations are used in model building as all are used in validation, ensuring all variability in the observations is used in both stages. Internal validation was used in the pilot.

The most successful model was achieved using the covariates listed in Table 1 and set to apply a 80/20 model build/validation split using the 22 site observations of AWC. The model build was repeated 50 times. In terms of mapping reliability, the model achieved a R^2 of 0.35 and a concordance correlation coefficient of 0.55. Concordance is perhaps the most informative quality metric because it reports the model quality in terms of the 1 to 1 observation/model result (Lin, 1989). A concordance value of 0.55 suggests a moderately strong model. The results for each 0.1 m depth 'slice' AWC are presented in Figure 6 and Figure 7. A whole of profile AWC (to 1 m depth) (Figure 7) was created in the GIS by combining the 0.1 m depth increment AWC layers.

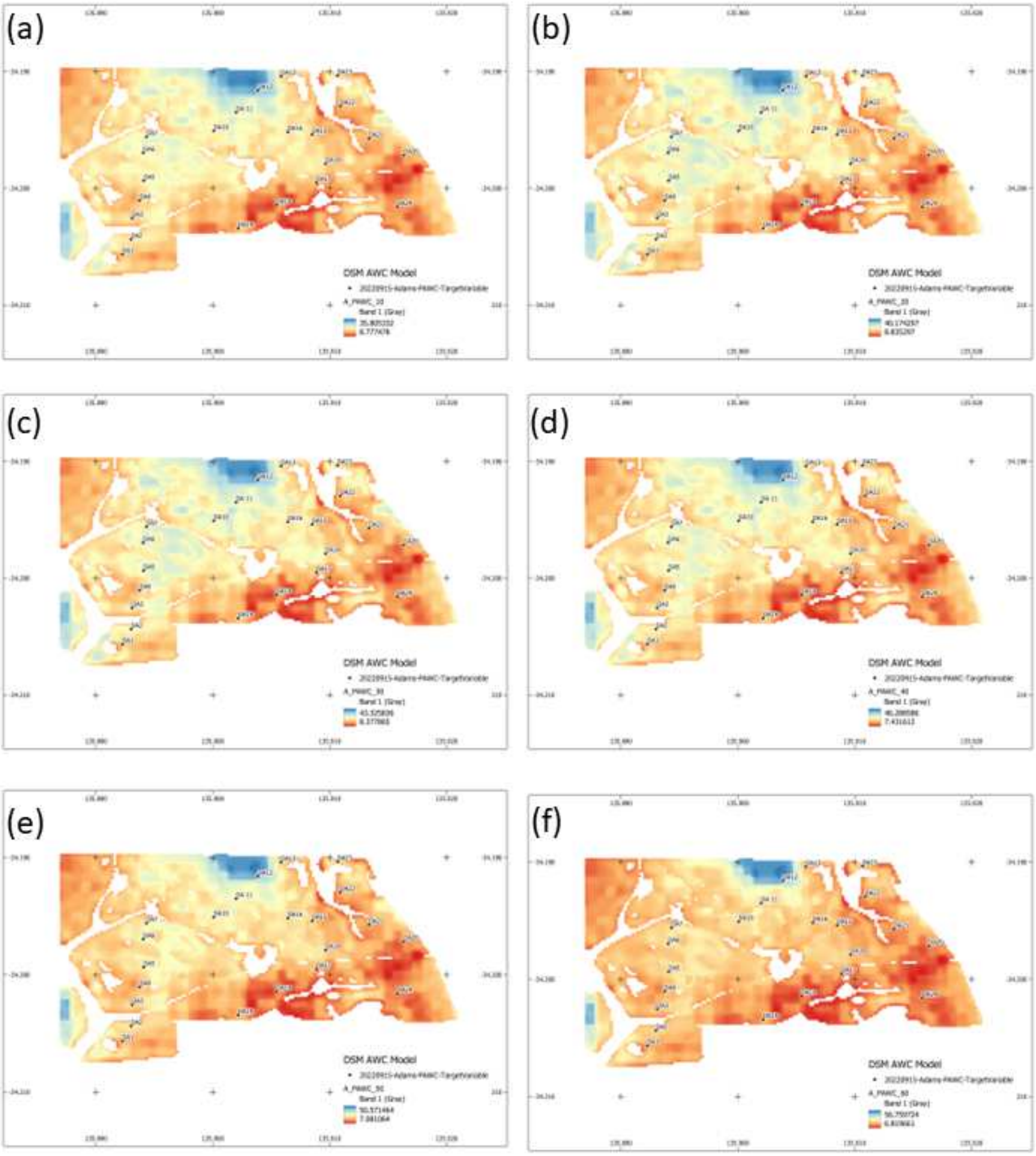

Figure 6. AWC predictions at various depth increments: (a) 0 - 01 m, (b) 0.1 – 0.2 m, (c) 0.2 – 0.3 m, (d) 0.3 – 0.4 m, (e) 0.4 – 0.5 m, and (f) 0.5 – 0.60 m

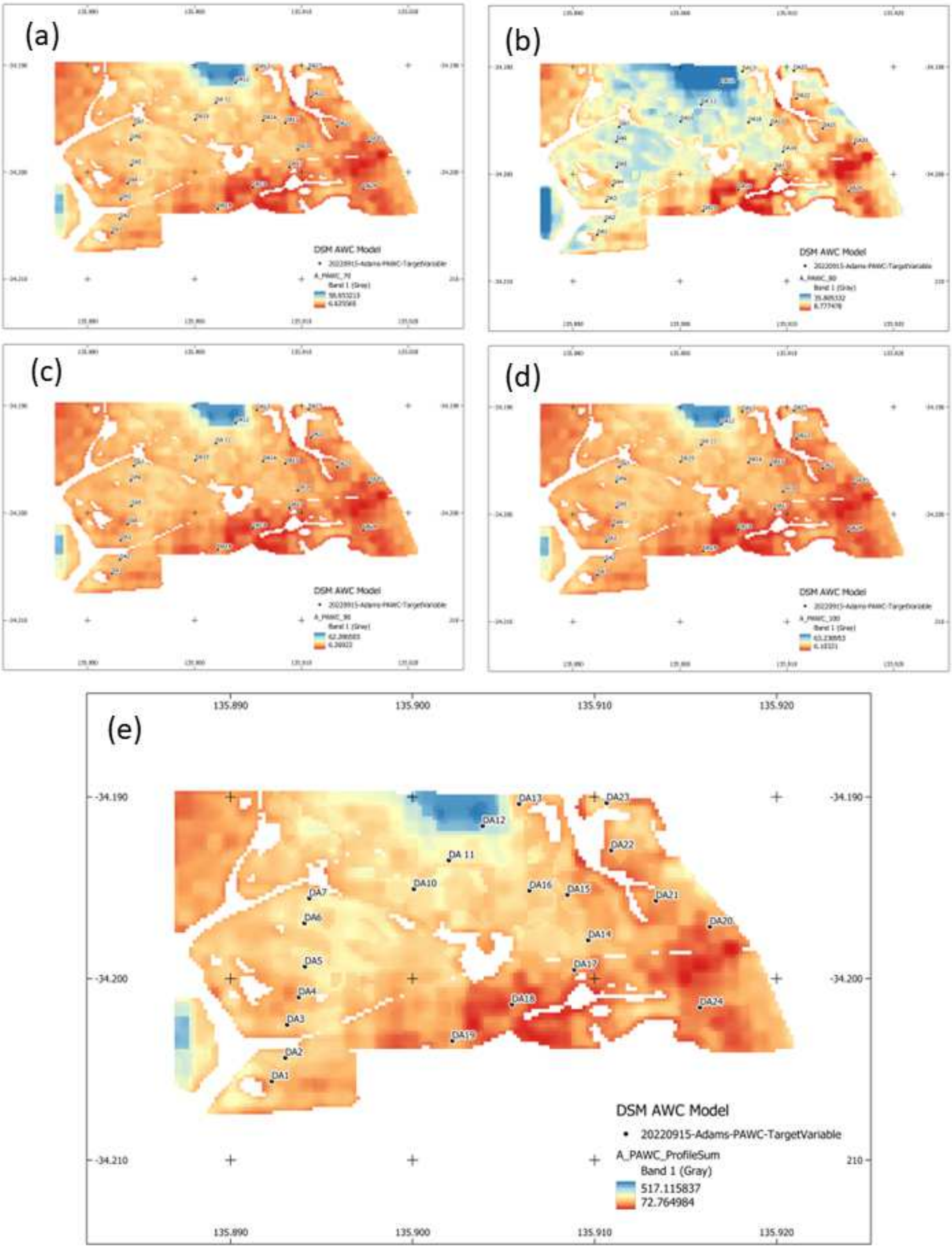

Figure 7. AWC predictions at various depth increments: (a) 0.6 – 0.7 m, (b) 0.7 – 0.8 m, (c) 0.8 – 0.9 m, (d) 0.9 – 1.0 m, and (e) Whole profile to 1 m

The Figures show that the depth slice predictions are in the range from approximately 6 mm to 60 mm AWC. Visually the figures show consistency in AWC patterns through the depth slices. The mapped zone with the greatest AWC is located that the centre of the northern boundary of the farm near site DA12. Figure 8 shows the traces created from the intersection of DSM depth slices at the sampling sites (also the model training sites). The DSM AWC trace at DA12 indicates a large and increasing AWC values down the profile, and an AWC profile form unlike any other of the plots. Lower AWC values are associated with the south and eastern farm zones where there were shallow soils were observed at DA19, DA21 and DA22. Figure 7 (b) shows that there is a consistent increase in AWC in the 0.7 – 0.8 m depth slice across the farm. The whole profile AWC shown in Figure 7 (e) shows the range of AWC values in the 70 – 520 mm range. Notably, mapped whole profile AWC values >350 mm (Figure 7 (e)) are unrealistic, especially given the analysis in this pilot is limited to 1 m deep soils. The DSM modelling to produce the unlikely profile form and AWC size represented at DA12 in Figure 8 is a good example of where the model has not performed well.

Figure 8. Comparison of down profile DSM and laboratory AWC values

Figure 8 shows the DSM traces are 'generalised' down-profile compared to the laboratory traces. The variance between the DSM and laboratory data at each depth increment (*n* = 201) is also summarised in the scatter plot in Figure 9, which shows a very weak correlation (R^2 = 0.043) between the two datasets. This weak relationships follow in Figure 8 with the DSM derived traces being generalised (i.e. straighter) down profiles. The DSM traces reflect that many soils had lighter textures (i.e. smaller AWC) in topsoils with heavier clayey subsoils.

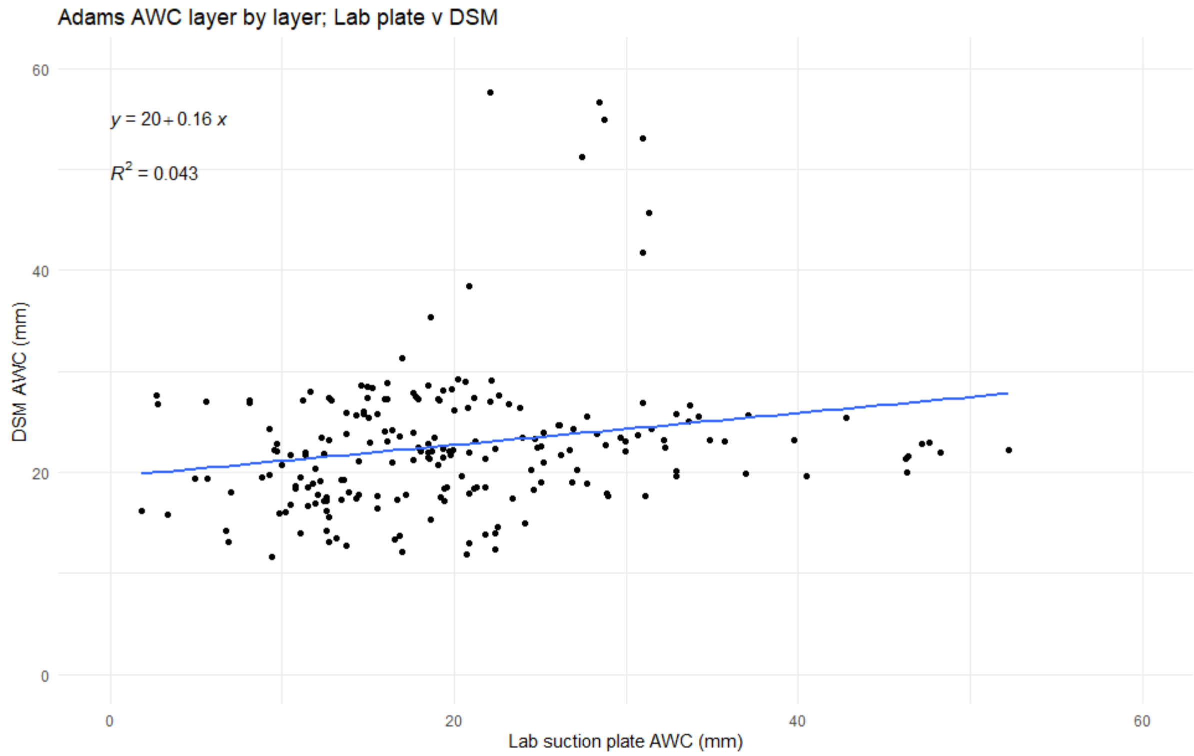

Figure 9. Scatter plot comparing predicted DSM AWC values against laboratory AWC values from each site and depth layer

Extrapolating moisture signal

The final phase of the pilot involved testing the use of signal from the Tank soil moisture probe to predict the AWC elsewhere on the farm at various times from the DSM. This method works under the premise that soil moisture information from the soil moisture probe reflects the contemporary soil moisture status across the farm, and rainfall received does not vary to a significant degree over the farm. Soil moisture data from periodic samplings at 11 predetermined sites on the farm has been used to evaluate the extrapolation.

Soil probe data

Soil moisture has been collected at the Adams probe since 2016 and the probe was changed during March 2022. The cumulative soil moisture to 1 m depth for the period it was functioning is shown in Figure 10, accompanied by rainfall distributions from the nearby Yeelanna rainfall station. The soil moisture trace reflects quite well contribution of seasonal patterns of rainfall, noting however a separation of approximately 15 km between the farm and rainfall station and the influence on distance between the two.

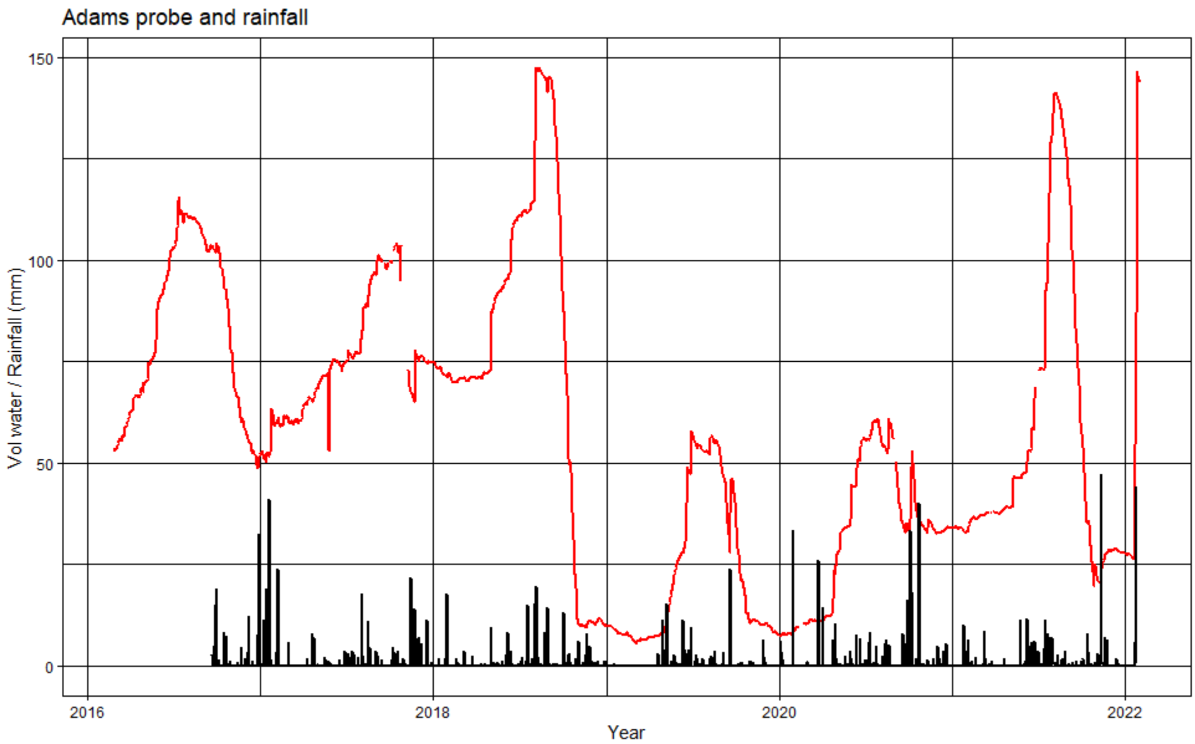

Figure 10. Adams probe soil moisture estimation (to 1 m) to February 2022 (red trace) and rainfall from the nearby Yeelanna rainfall station (black trace)

Soil moisture sampling

Soil moisture measurements were collected at various depths increments (0 – 0.1, 0.1 – 0.2, 0.2 – 0.4, 0.4 – 0.6, 0.6 – 0.8, and 0.8 – 1.0 m) from 11 fixed locations on the farm shown in Figure 11. These sites were sampled during 11 May 2021, 30 September 2021, and 2 February 2022 and moisture measurements made in the laboratory. These were converted to volumetric soil measurements for each depth increments using bulk density estimates derived through GIS intersection of the bulk density mapping from the SLGA.

Figure 11. Periodic soil moisture sampling sites (white dots) and DSM sampling sites (red dots)

Using the soil moisture probe to modify DSM AWC

Whole farm whole profile (1 m) water at soil moisture sampling dates was estimated by applying the contemporary Tank probe signal to the whole farm AWC DSM in Figure 7 (e). This modifier was derived from a normalised[3] multiplier and applying the modifier from the date to the AWC DSM. Figure 12 shows a comparison on values taken from soil moisture sampling sites in Figure 11. The comparisons are shown in Figure 12, which shows a weak relationship (R^2 = 0.19, all dates combined) between the field soil moisture measurements and modified AWC.

[3] (x – minimum)/range, values of 0 - 1

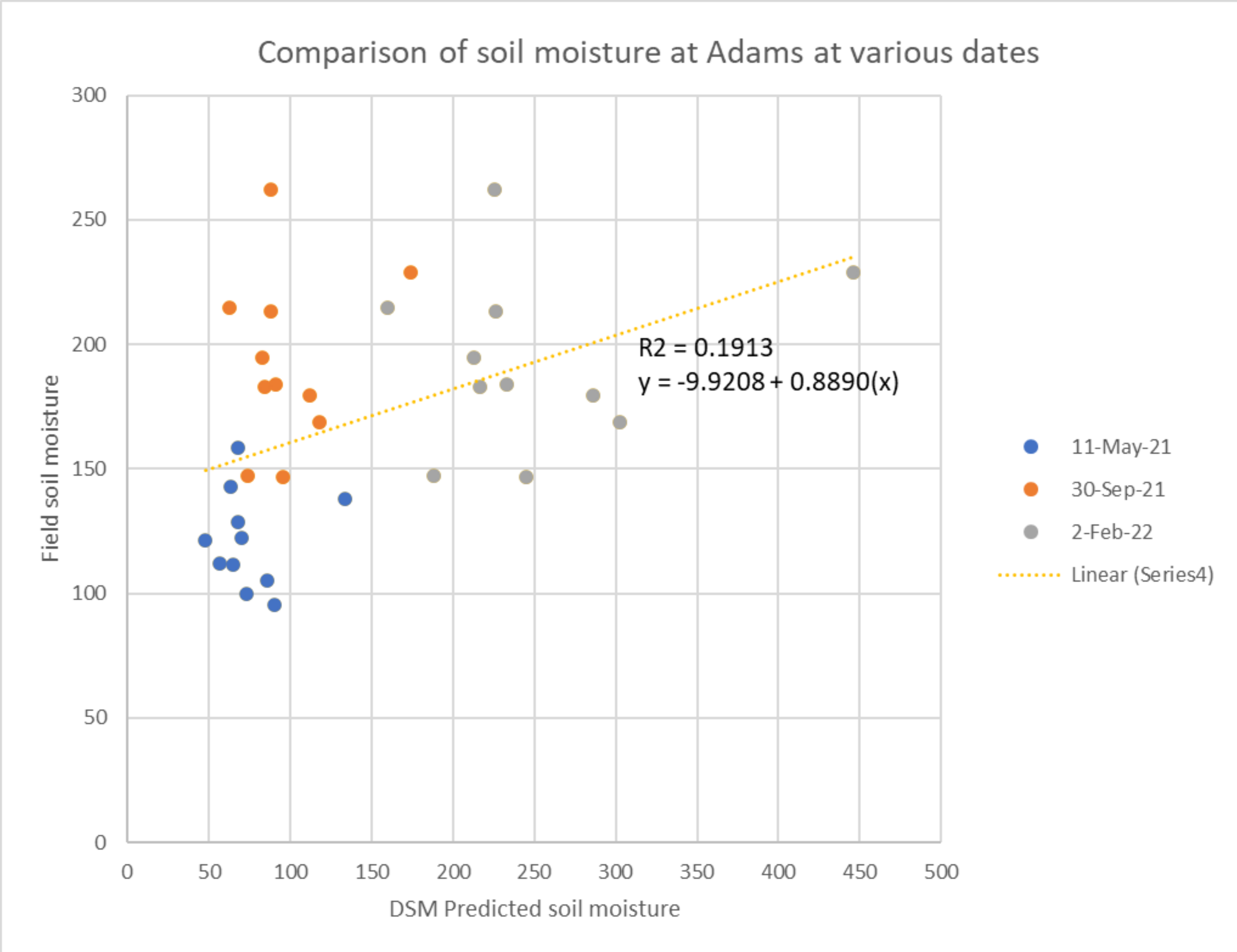

Figure 12. Scatter plot comparing modified soil moisture from DSM AWC with soil moisture from field sampling. The three dates are shown and best fit line for combined date comparisons

Conclusions and recommendations

The pilot project applied soil-landscape principles to formulate a non-bias and efficient soil sampling design to survey the Adams farm. The soils were sampled at 22 sites at both 0.1 and 0.2 m increments to 1 m depth. Using laboratory methods available water capability (AWC) was measured for each 0.1 m depth increment.

The 10 cm AWC increments were used to model AWC for the whole farm at a 20 m ground resolution using computer machine learning digital soil mapping (DSM). Based on the soil survey intensity alone, this mapped output is consistent with a semi-detailed intensity of soil survey, which equates to approximately 1:25,000 scale mapping, placing the utility of output at the end range of moderately intensive uses at “field level” according to Gallant et al. (2008). While this may not support tactical farm decision-making one would expect at the level of precision agriculture (Jochinke et al., 2007), the AWC map gives an appreciation of within paddock variation offering a new level of farmer support/appreciation/understanding - and of course inter-paddock variation. The model delivered a Lin’s coefficient of correlation of 0.55 indicating a moderately strong model for AWC across the farm. However, when the 0.1. m AWC increments were compared with the laboratory data it was found that there was weak relationship (R^2 = 0.043).

The Tank probe soil moisture data was used to predict whole farm soil moisture at times corresponding to various field measurements of soil moisture. This was done by normalising the probe data at a 0 – 1 range, and applying the modifier from the sampling date to the whole of farm DSM AWC mapping. A weak relationship (R^2 = 0.19) was found.

In conclusion, by any measure, the reliability of outputs from each stage of the pilot study have been variable. There are several ways that errors could be addressed at each of the important stages, including assurance that:

- The soil survey design was not optimal, and not all representative soils were sampled.
- The DSM approach was not optimised well; other user configurations and approaches could be tested.
- The SLGA covariates that were used for DSM prediction were not capable of adequately representing covariance in soils. This may be a factor of thematic quality of the SGLA layers or a mismatch between native raster resolution and inherent soil variability.
- The Tank soil moisture probe has had known problems and was replaced once during the span of the study. The probe may also have been placed in a soil that for one reason or another does not represent well the soil moisture dynamics of the other farm soils.

Acknowledgements

We expressly acknowledge Dan Adams of access to his land and discussions had, Dr Rob Bramley (CSIRO) for useful comment, and Christina Ratcliff (CSIRO) for her ever-ready support around project data resources and GIS.

References

Burrough, P.A., 1989. FUZZY MATHEMATICAL-METHODS FOR SOIL SURVEY AND LAND EVALUATION. Journal of Soil Science 40(3), 477-492.

Cresswell, H.P., 2002. The soil water characteristic. In: D.C. McKenzie, K. Coughlan, H.P. Cresswell (Eds.), Soil physical measurement and interpretation for land evaluation. CSIRO Publishing, Collingwood, pp. 59 - 84.

Gallant, J., Austin, J., 2012. Topographic Wetness Index derived from 1" SRTM DEM-H. Canberra.

Gallant, J.C., McKenzie, N.J., McBratney, A.B., 2008. Scale. In: N.J. McKenzie, M.J. Grundy, R. Webster, A.J. Ringrose-Voase (Eds.), Gudelines for Surveying Soils and Land Resources. CSIRO Publishing, Melbourne, pp. 27-43.

Grundy, M.J., Rossel, R.A.V., Searle, R.D., Wilson, P.L., Chen, C., Gregory, L.J., 2015. Soil and Landscape Grid of Australia. Soil Research 53(8), 835-844.

Hall, J.A.S., Maschmedt, D.J., Billing, N.B., 2009. The Soils of Southern South Australia. Department of Water, Land and Biodiversity Conservation, Government of South Australia, Adelaide, Australia.

Jochinke, D.C., Noonon, B.J., Wachsmann, N.G., Norton, R.M., 2007. The adoption of precision agriculture in an Australian broadacre cropping system—Challenges and opportunities. Field Crops Research 104(1), 68-76.

Lin, L.I., 1989. A concordance correlation-coefficient to evaluate reproducibility. Biometrics 45(1), 255-268.

Maschmedt, D., 2000. Assessing agricultural land: agricultural land classification standards used in South Australia's land resource mapping program, Primary Industries and Resources South Australia, Adelaide, Australia.

McBratney, A.B., Santos, M.L.M., Minasny, B., 2003. On digital soil mapping. Geoderma 117(1-2), 3-52.

McKenzie, N.J., Ryan, P.J., 1999. Spatial prediction of soil properties using environmental correlation. Geoderma 89(1-2), 67-94.

McKenzie, N.J., Webster, R., Ryan, P.J., 2008. Sampling using statistical methods. In: N.J. McKenzie, M.J. Grundy, R. Webster, A.J. Ringrose-Voase (Eds.), Guidelines for surveying soil and land resources. CSIRO Publishing, Collingwood, Vic., pp. 319-326.

Prescott, J.A., 1950. A climatic index for the leaching factor in soil formation. Journal of Soil Science 1(1), 9-19.

Ratcliff, C., Gobbett, D.L., Bramley, R., 2020. PAT - Precision Agriculture Tools. CSIRO.

Torres, R., Snoeij, P., Geudtner, D., Bibby, D., Davidson, M., Attema, E., Potin, P., Rommen, B., Floury, N., Brown, M., Traver, I.N., Deghaye, P., Duesmann, B., Rosich, B., Miranda, N., Bruno, C., L'Abbate, M., Croci, R., Pietropaolo, A., Huchler, M., Rostan, F., 2012. GMES Sentinel-1 mission. Remote Sensing of Environment 120, 9-24.

Wilford, J., 2012. A weathering intensity index for the Australian continent using airborne gamma-ray spectrometry and digital terrain analysis. Geoderma 183, 124-142.

Wilford, J.R., Bierwirth, P.N., Craig, M.A., 1997. Application of airborne gamma-ray spectrometry in soil/regolith mapping and applied geomorphology. AGSO Journal of Australian Geology & Geophysics 17(2), 201 - 216.

Wilson, J.P., Gallant, J.C., 2000a. Digital terrain analysis. In: J.P. Wilson, J.C. Gallant (Eds.), Terrain analysis: principles and applications. John Wiley & Sons Inc., New York, pp. 1-27.

Wilson, J.P., Gallant, J.C., 2000b. Secondary Topographic Attributes. In: J.P. Wilson, J.C. Gallant (Eds.), Terrain analysis: principles and applications. John Wiley & Sons Inc., New York, pp. 87-131.

Appendix 1

Gravimetric moisture contents of soil profiles to 1 m depth (or core refusal) from laboratory pressure and suction plate analyses. Red line approximates crop lower limits (CLL) and blue line, the drained upper limit (DUL).

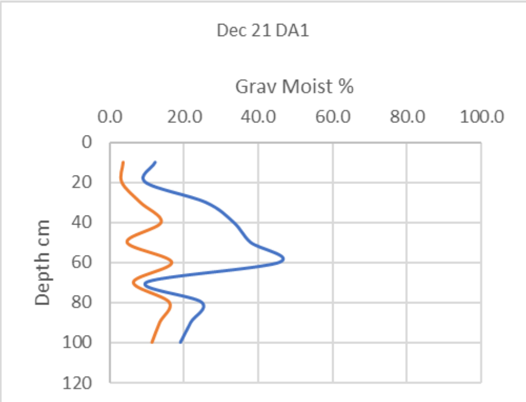

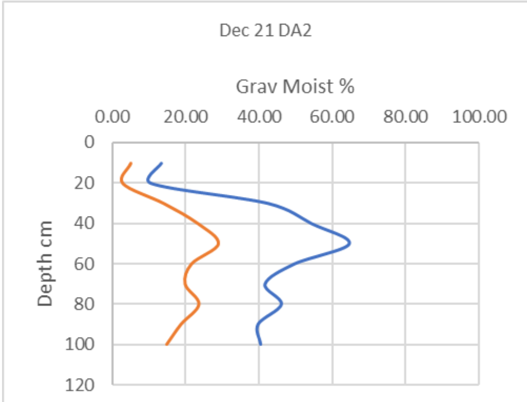

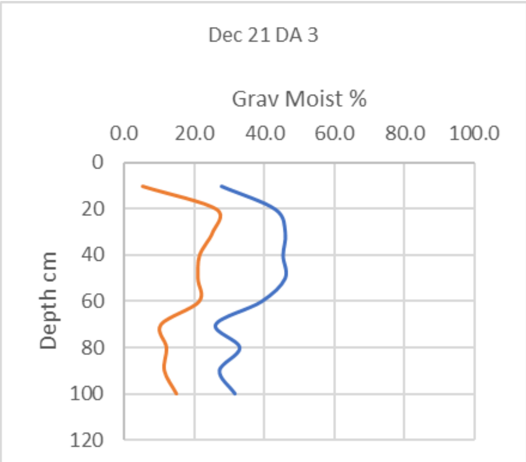

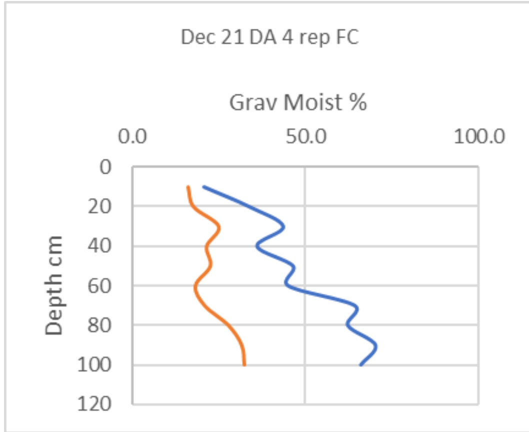

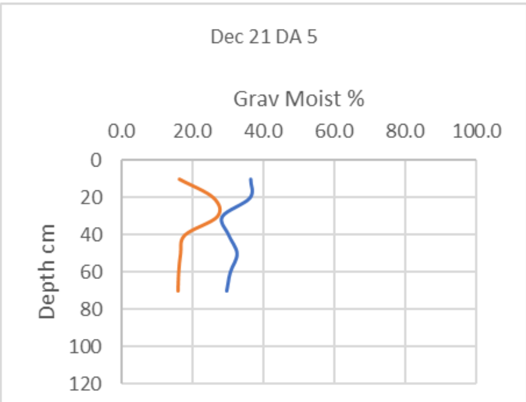

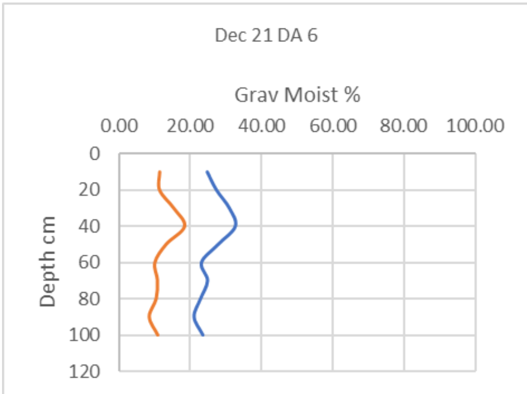

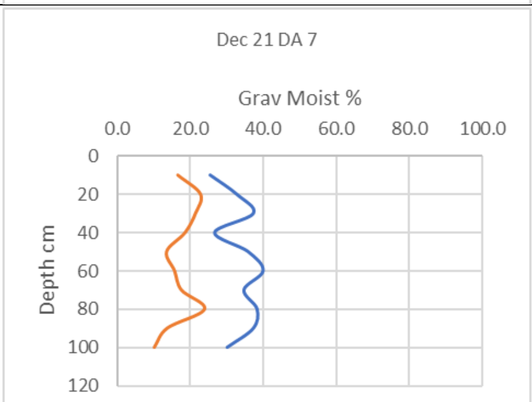

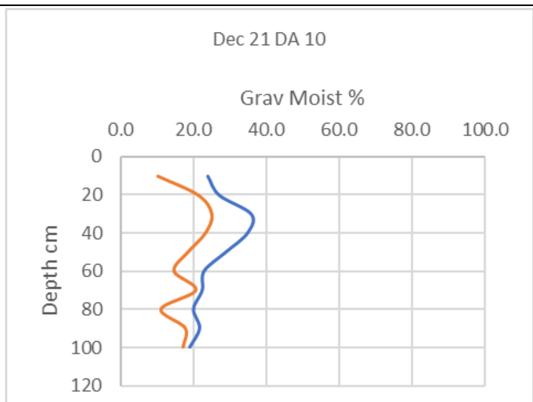

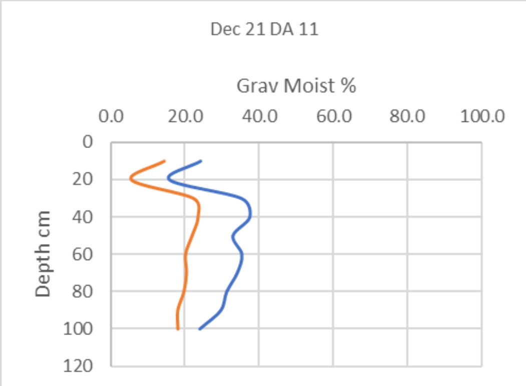
Dec 21 DA 11
Grav Moist %
0.0 20.0 40.0 60.0 80.0 100.0
Depth cm
0 20 40 60 80 100 120

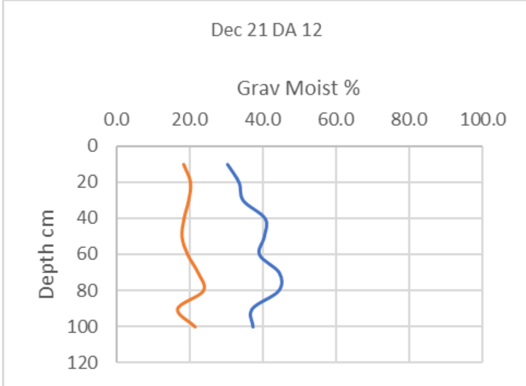
Dec 21 DA 12
Grav Moist %
0.0 20.0 40.0 60.0 80.0 100.0
Depth cm
0 20 40 60 80 100 120

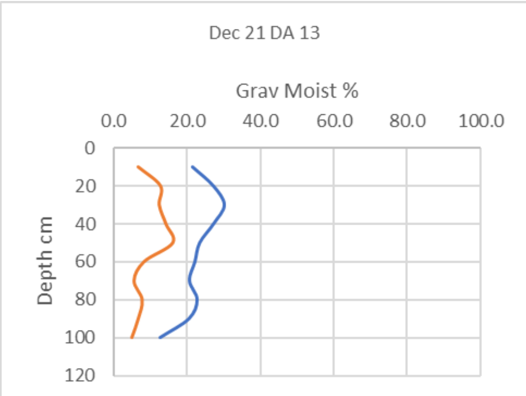
Dec 21 DA 13
Grav Moist %
0.0 20.0 40.0 60.0 80.0 100.0
Depth cm
0 20 40 60 80 100 120

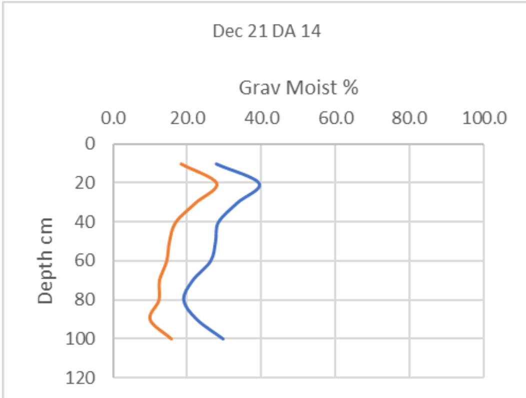
Dec 21 DA 14
Grav Moist %
0.0 20.0 40.0 60.0 80.0 100.0
Depth cm
0 20 40 60 80 100 120

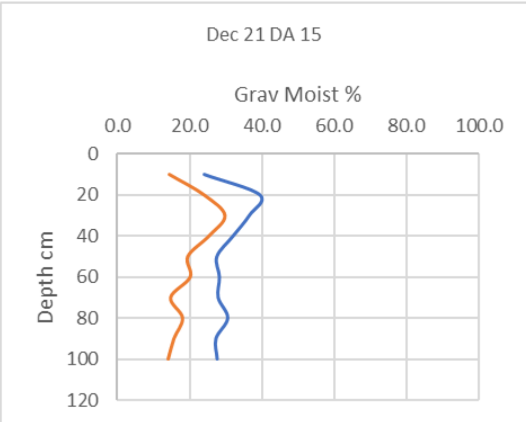
Dec 21 DA 15
Grav Moist %
0.0 20.0 40.0 60.0 80.0 100.0
Depth cm
0 20 40 60 80 100 120

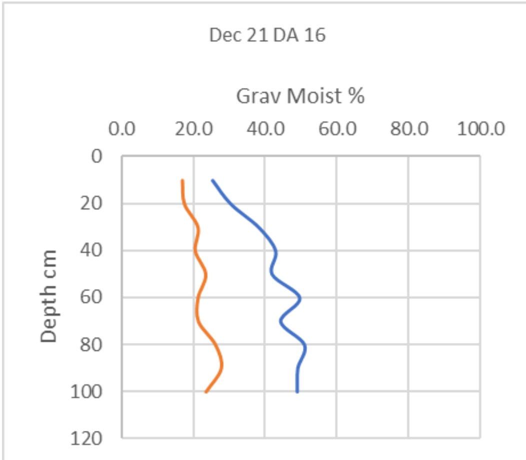
Dec 21 DA 16
Grav Moist %
0.0 20.0 40.0 60.0 80.0 100.0
Depth cm
0 20 40 60 80 100 120

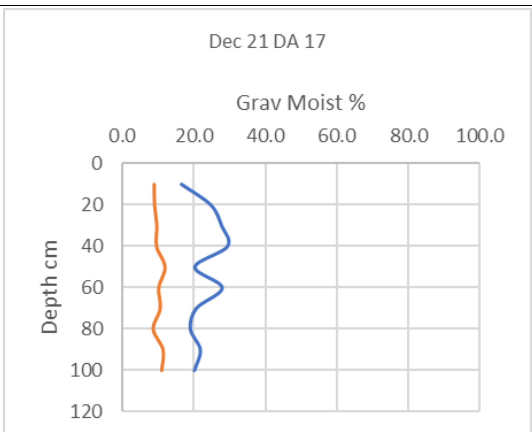
Dec 21 DA 17
Grav Moist %
0.0 20.0 40.0 60.0 80.0 100.0
Depth cm
0 20 40 60 80 100 120

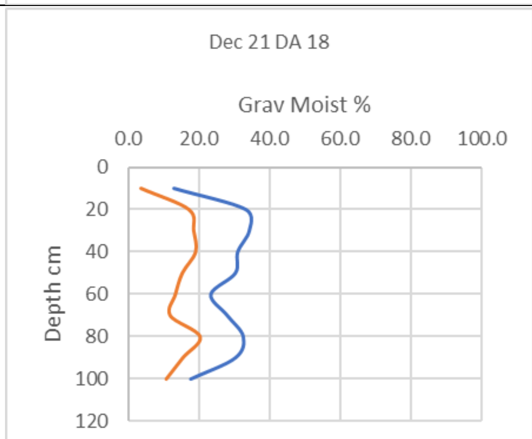
Dec 21 DA 18
Grav Moist %
0.0 20.0 40.0 60.0 80.0 100.0
Depth cm
0 20 40 60 80 100 120

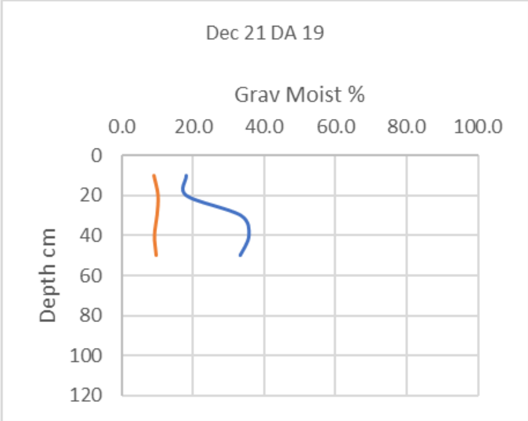

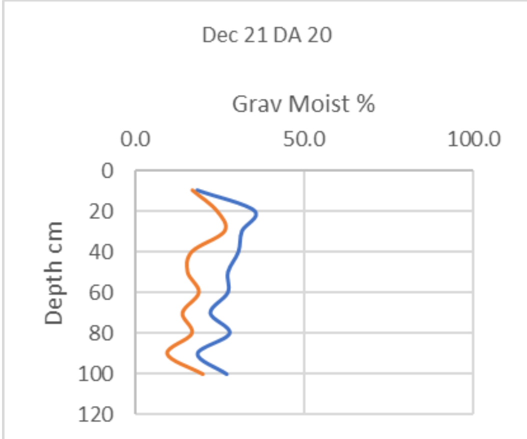

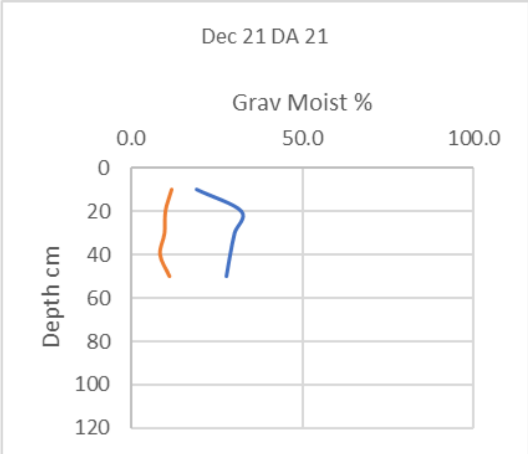

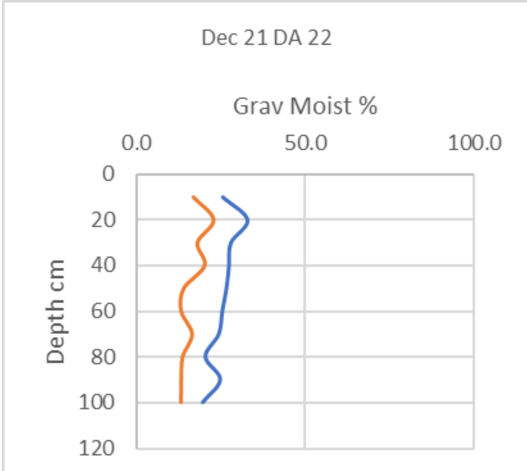

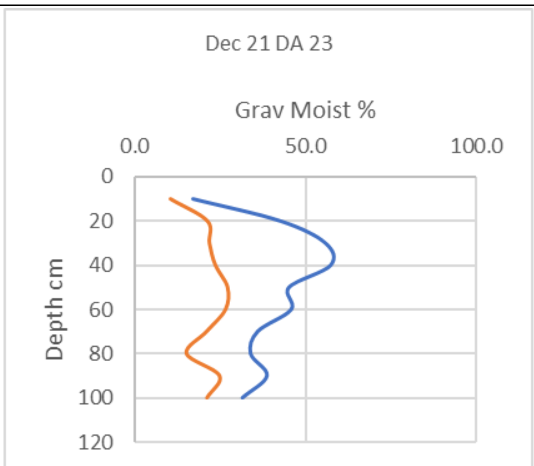

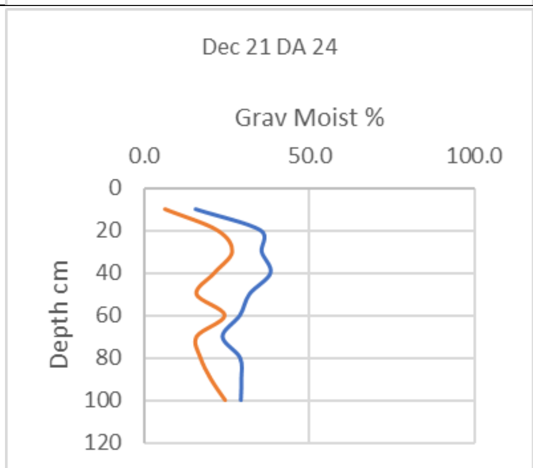

Project Funders
Australian Government
National Landcare Programme
Project Proponents
AIR EP Ag Innovation & Research Eyre Peninsula
Project Partners
CSIRO Regional Connections SARDI SquareV EPAG COUTTS J&R